RESEARCH ARTICLE

INTERNATIONAL RESEARCH JOURNAL OF MULTIDISCIPLINARY TECHNOVATION

Asian Research Association

DOI: 10.54392/irjmt25611

Integration of Model Free Kinetics and Machine Learning to Evaluate the Thermal Stability Behaviour of Nano Enhanced Composite Phase Change Materials

K. Pavan Kumar [a, b, *], T.V.K. Bhanu Prakash [a], Aditya Mukherjee [c]

[a] Department of Marine Engineering, Andhra University, Visakhapatnam, 530003, Andhra Pradesh, India
[b] MVGR College of Engineering(A), Vizianagram, 535005, Andhra Pradesh, India,
[c] Department of Chemical Engineering, GVP College of Engineering, Visakhapatnam-530048, Andhra Pradesh, India
* Corresponding Author Email: pavankmech@gmail.com

DOI: https://doi.org/10.54392/irjmt25611
Received: 17-06-2025; Revised: 27-10-2025; Accepted: 04-11-2025; Published: 15-11-2025

Abstract: The phase change materials (PCMs) used in medium-temperature thermal energy storage can store and release a large amount of latent heat. However, their use in real-world applications is often limited by poor thermal conductivity and degradation stability during repeated heating cycles. Therefore, improving the thermal reliability and kinetic behaviour of PCMs is essential for advancing high-performance energy storage systems. This research assessed the thermal stability and degradation kinetics of pure D-mannitol and its graphene nanoplatelet (GNP)-reinforced composites. It introduced a new combination of model-free kinetic modelling and machine-learning-based predictions for evaluating the thermal reliability of nano-enhanced PCMs. Five different PCM compositions (containing 0, 0.25, 0.5, 0.75, and 1 wt% GNP) were prepared using ultrasonic-assisted dispersion. Non-isothermal thermogravimetric analysis (TGA) was performed at five different heating rates (10–25 °C·min^{-1}), and the activation energies (E_a) were determined using the Kissinger–Akahira–Sunose (KAS), Flynn–Wall–Ozawa (FWO), and Starink model-free methods. The Starink model yielded the lowest E_a for pure D-mannitol (61.99 kJ·mol^{-1} at $\alpha \approx 0.1$), while the KAS and FWO models provided mean values of 137.62 kJ·mol^{-1} and 141.48 kJ·mol^{-1}, respectively. Incorporating GNP improved thermal stability across all compositions, with E_a ranging from 123.67 to 149.08 kJ·mol^{-1}. The random forest regression model achieved the best predictive accuracy ($R^2 = 0.99$, RMSE = 0.0002), outperforming both linear and polynomial models. Overall, the addition of graphene nanoplatelets significantly enhances both chemical and thermal stability, confirming their role as effective nano-additives for PCM improvement and enabling the design of thermally stable “smart” energy storage systems for solar and sustainable applications. The thermal stability of Graphene Nanoplatelets (GNP)-enhanced D-Mannitol was determined through non-isothermal TGA analysis at heating rates between 10–25 °C min-1. The decomposition behaviour of the GNP-enhanced D-Man was characterized using Model-Free Kinetic Methods and Machine Learning Models to determine the accuracy of predicting the thermal stability of the D-Man using the most significant thermal parameters.

Keywords: D-Mannitol, Graphene Nano platelets, Thermal Decomposition, Activation Energy, Machine learning

1. Introduction

Phase change materials (PCMs), which are an important part of thermal energy storage, are materials that have a change in phase from solid to liquid or vice versa and can absorb (or release) large amounts of heat through this process [1]. The problem with using PCMs as a form of thermal energy storage is that they have limited thermal degradation potential at medium temperatures, especially if they are nano-materials enhanced to improve thermal energy properties. Research has been published about the thermal degradation of nano-enhanced PCMs and strategies to limit that degradation [2]. Furthering the practical application of PCMs in energy storage devices by identifying ways to lower thermal degradation will lead to additional research regarding strategies to increase the thermal stability and performance of PCMs. Improved thermal stability and performance of PCMs make them an attractive option to consider as part of a solution for managing thermal energy.

Yang *et al.* (2018) found that when CNTs are added to a paraffin-based PCM, this reduces degradation by increasing thermal stability through enhanced heat conduction [3]. Sharma et al. (2018) also showed that GNP’s increased both thermal conductivity and oxidative stability of fatty acid based PCMS in the

mid temperature range. Several studies have also shown that nanoparticles such as nanoclay, carbon material, and metal oxides can improve PCM performance [4]. Aqib *et al.* (2020) observed an improvement in both heat transfer capacity and thermal stability of eutectic salts with the addition of nanostructured Al_2O_3 [5]. Zhang *et al*. (2020) also found that GO nanosheets delay the degradation of PEG at elevated temperatures due to their high thermal conductivity and O barrier properties [6]. This study demonstrates that nano-enhanced salt hydrate is suitable for solar-thermal energy storage systems which operate in the temperature ranges of 100 – 300°C.

Selecting appropriate phase-change materials (PCMs) for thermal energy storage applications involves several factors, including thermal stability. Thermal stability is generally assessed by employing thermogravimetric analysis (TGA), which measures the degradation of a material when heated. The TGA can provide important degradation characteristics that reflect a PCM's thermal stability, such as the degradation rate of the PCM and the percent weight loss of the PCM at specified temperatures. TGA allows researchers to establish degradation kinetics under different heating conditions. As reaction rates are extremely temperature dependent, activation energy is a significant measure of thermal stability, especially regarding nano-enhanced PCMs. There are several kinetic models available to evaluate non-isothermal TGA data for organic and inorganic substances that undergo thermal decomposition [7].

Integrated model-free techniques (KAS, FWO, Starink) provide an efficient way to assess both activation energy and degradation kinetic parameters, creating a complete tool for evaluating PCM thermal durability [8]. The application of these integrated techniques is widespread for identifying degradation pathways and quantifying activation-energy variation caused by nano-enhancements that can impact a material's dependability and longevity [9]. For example, Venkitaraj *et al*. (2019) utilized the KAS technique to evaluate nano-enhanced solid-solid PCMs and determined that the addition of aluminium oxide nanoparticles reduced the activation energy from 123 kJ/mol to 98 kJ/mol [10]. In another study, Xiang et al. (2019) evaluated shape-stable PCMs containing polymer membranes via the FWO technique; they identified that polypropylene membranes demonstrated the greatest activation energy (99.30 kJ/mol), corresponding to the greatest thermal durability at 50 % conversion [11].

Data-driven models offer efficient and accurate prediction of thermal behaviour in energy systems [12]. Bhamare *et al.* (2021) showed that hybrid ML improved nano-PCM stability and capacity [13], while Basem et al. (2025) used regression and neural networks to predict NEPCM degradation [14, 15]. Advanced models such as SVR and ANN optimized degradation trends using TGA inputs [16]. Singh *et al.* (2023) confirmed that nanoparticle type, heating rate, and dispersion uniformity govern thermal stability and activation energy in nano-enhanced PCMs [17].

Support Vector Machine (SVM) has gained attention for its strong predictive capability in complex datasets [18]. Dong *et al*. (2005) and Wei et al. (2015) demonstrated its superior accuracy in minimizing prediction errors and forecasting urban energy demand [18, 19]. Bagheri-Esfeh et al. (2020) applied the GMDH method to optimize PCM performance in building heating and cooling, achieving $R^2 > 0.9$ [20]. Similarly, Bhamare *et al.* (2020) reported that ANN models provided the best thermal prediction accuracy ($R^2 >$ 96%), confirming the reliability of ML algorithms in PCM-based energy applications [21].

Recent open-access studies by Said *et al.* (2024) and Xiao *et al*. (2023) proposed innovative strategies to enhance the stability and durability of nano-enhanced PCMs [2, 22]. These works also integrated machine learning with PCM wall simulations to optimize thermal storage performance. However, none combined model-free kinetic methods (KAS, FWO, Starink) with data-driven predictive modelling for D-mannitol/GNP composites. This study uniquely integrates kinetic parameter estimation and ML regression to predict thermal degradation, advancing PCM design and performance optimization.

Previous studies found that the addition of nanoparticles (CNTs, Al_2O_3, GO) enhanced heat transfer and thermal oxidation stability of phase change materials (PCMs). Nonetheless, existing literature is inconsistent for a variety of reasons; the type of additive, the quantity of additive, and the specific base PCM utilized were all variables. For instance, metallic oxide additives typically lower the activation energy, while carbon based additives like graphene enhance both electrical conductivity and degradation resistance via barrier and phonon transport effects. Most of the studies conducted previously used either paraffin or salt-hydrate as the base PCM and very rarely investigated sugar-alcohols like D-mannitol, which undergo different decompositions. Additionally, few investigations have correlated machine learning predictions with kinetic model parameters (KAS, FWO, Starink) to determine if the degradation behaviours are valid.

Thus, the present research addresses both of these shortcomings through (i) conducting a consistent kinetic evaluation of D-mannitol/GNP composite materials using standard TGA testing methodologies, and (ii) integrating the determination of kinetic parameters with a machine-learning-based predictive model in order to understand degradation processes better and provide an accurate means of predicting stability for medium-temperature TES systems.

While numerous investigations have focused on PCMs, there is a lack of an inclusive analysis of the thermal and kinetic stability of nano-enhanced D-mannitol. The current research provides a gap in the literature by providing a systematic investigation of the degradation kinetics of both pure and GNP-enhanced D-mannitol under non-isothermal TGA conditions (10-25°C min−1) utilizing model free methods (KAS, FWO, Starink) [2]. It is anticipated that graphene nanoplatelets will enhance thermal stability due to enhanced heat transfer as well as a barrier effect of GNPs; however, inconsistent activation energy trends between the reviewed studies emphasize the necessity for a unifying framework. To provide such a framework, the current work combines kinetic models with machine learning based predictions/uncertainty assessment to provide a valid method for developing thermally-stable PCMs for use in TES systems at intermediate temperatures [3, 4].

2. Experimental procedure

2.1 Material Selection through the Analytic Hierarchy Process (AHP)

The selection of suitable phase change materials (PCMs), for medium temperature applications used in areas that include thermal energy storage and solar energy generation; the relevant material properties are identified in Table 1, is a critical component to achieve the goal of high latent-heat capacity, good thermal stability, cost-effective and low environmental impact [23].

The Analytic Hierarchy Process (AHP) was developed to be a systematic approach to multi-criteria decision making to help in evaluating and selecting the best possible phase-change materials (PCMs). The normalized weights for the criteria and the consistency ratio for each criterion are listed in Table 2.

Using AHP, alternatives (i.e., PCMs) are evaluated with respect to various criteria latent heat of fusion, thermal conductivity, cost and environmental influence by developing a hierarchical model [23,24] and comparing them through a series of pair-wise comparisons that are then synthesized into an overall ranking of the most applicable PCM for the specific thermal application being studied [24].

In order to provide a transparent and reproducible process, Table 1 includes the entire pairwise comparison matrix of the latent heat criterion. Additionally, Table 2 contains both the normalized criteria weights as well as the consistency ratio (CR = 0.07, which meets Saaty's requirement that CR < 0.10 to validate the logical consistency of the pairwise comparisons).

The Candidate PCMs Final Ranking Scores are shown in Table 3; The Comparative Weighted AHP Results are graphically illustrated as a bar chart (Figure 1) showing that the D-Mannitol has the Highest Suitability Score compared to all other Materials [25].

Table 1. Pairwise-Comparison Matrix for Latent Heat Criterion

Material	|D-Mannitol	Erythritol	Lithium Nitrate	Solar Salt	Penta Erythritol	Priority Weight
D-Mannitol	1	2	4	6	8	0.38
Erythritol	0.5	1	3	5	6	0.27
Lithium Nitrate	0.25	0.33	1	3	4	0.15
Solar Salt	0.17	0.2	0.33	1	2	0.11
Penta Erythritol	0.13	0.17	0.25	0.5	1	0.09

Table 2. Normalized Criteria Weights and Consistency Ratio (CR)

Criterion	Weight	λ_{max}	CI	CR	Remark
Latent Heat	0.31	–	–	–	–
Thermal Conductivity	0.18	–	–	–	–
Cost	0.14	–	–	–	–
Specific Heat	0.12	–	–	–	–
Thermal Reliability	0.10	–	–	–	–
Safety	0.08	–	–	–	–
Environmental Impact	0.07	–	–	–	–
Overall	1.00	5.25	0.06	0.07 (<0.1)	Consistent

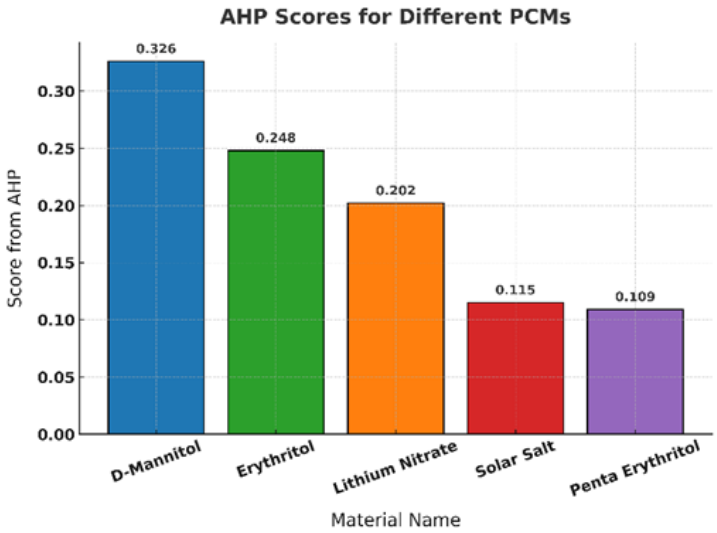

Figure 1. Comparison of candidate PCMs based on AHP-weighted scores identifying D-Mannitol as the optimal material for medium-temperature TES applications

Table 3. Selection and Prioritization of PCMs for Medium-Temperature Applications Using AHP

S.No	Material Name	Score from AHP
1	D-Mannitol	0.326
2	Erythritol	0.248
3	Lithium Nitrate	0.202
4	Solar Salt	0.115
5	Penta Erythritol	0.109

D-Mannitol was ranked highest in terms of Overall Suitability due to its High Latent Heat Capacity and Balancing Thermophysical Properties; Erythritol also performed very well, although slightly lower than D-Mannitol; Lithium Nitrate and Solar Salt contributed equally well to the total, while Penta Erythritol demonstrated the Lowest Total, thus indicating that this Material would be least desirable for Medium Temperature Applications [3-6].

2.2 Material preparation

D-Mannitol was determined by the AHP (Analytic Hierarchy Process) analysis (see Table 3), to be the most effective PCM. D-mannitol has high thermal stability and a large latent heat capacity; however, it also has a very low thermal conductivity, which may limit its ability to transfer heat effectively. Therefore, to improve the thermal conductivity and stability of the D-mannitol, Graphene Nanoplatelets (GNPs) were added to create a composite material [26]. The details of how the composite material was prepared can be seen in figure 2 and all of the information regarding the experimental materials used in the study is provided in table 4.

The initial steps included heating pure D-mannitol at 170°C; then adding GNPs (wt% 0.25–1) gradually while magnetically mixing until uniform particle distribution was achieved. To ensure complete uniformity, ultrasonic sonication was performed on the sample for 30 min [27]. Following that, the sample was heated in a muffle furnace to remove any air entrapment and to increase mechanical bonding between the matrix and fillers [28]. Finally, the solid composite was pressed into a disc for additional thermal testing. Details regarding the composition of each nano-PCM sample are listed in Table 5.

The amount of graphene nanoplatelets (GNPs), ranging from 0.25 to 1 wt %, was chosen because preliminary tests in other experimental studies involving sugar-alcohols as base materials for PCMs indicated that GNPs are effective at improving thermal conductivity and structure stability when added in low amounts less than 1wt %. However, it has been shown that preliminary experiments using higher weight percentages (greater than 1 wt%) of GNPs have resulted in a non-uniform distribution of GNPs within the composite, an increase in viscosity, and thus a reduction in both thermal reliability and thermal transfer uniformity. Therefore, the selected GNP range (0.25 wt% – 1.0 wt%), is considered the optimal amount of GNPs to provide the best balance of uniform dispersion of the GNPs throughout the composite, enhanced thermal transfer, and retained latent-heat capacity for composites containing D-mannitol.

Table 4. Experimental Materials and their Details

Material	Specifications	Purchase Location	Use in Experiment
Graphene Nano Powder	**Purity:** 99% **Size:** 10nm **CAS No:** 7732-42-5 **Form:** Very Light Powder	Bangalore	Investigating thermal conductivity and material stability under varying conditions
D-Mannitol	**CAS No:** 69-65-8 **EC No:** 200-711-8	Mumbai	Studying decomposition behaviour and thermal stability properties

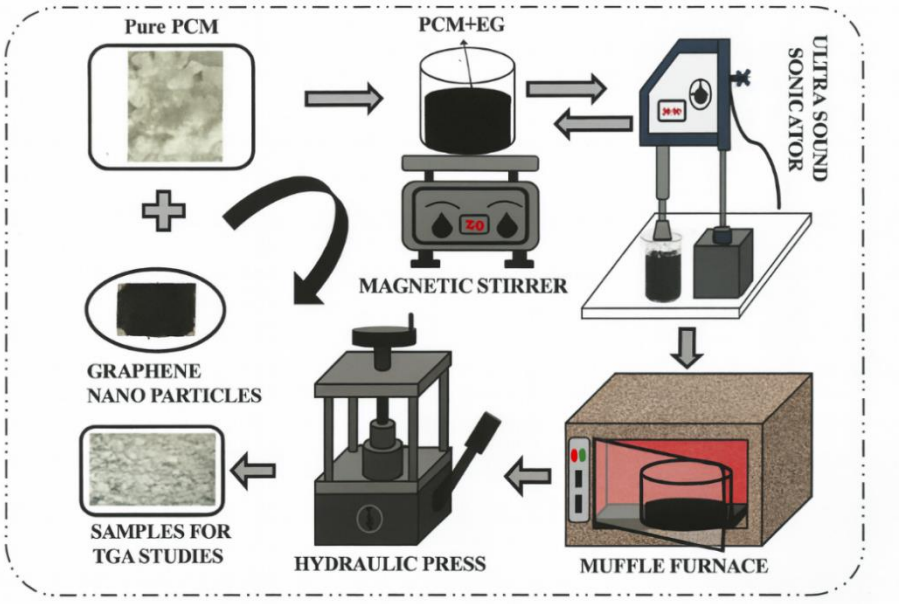

Figure 2. Schematic of the preparation steps for GNP-enhanced D-Mannitol PCM, including mixing, sonication, heat treatment, and hot pressing

Table 5. Nano PCM preparation using different weight compositions

S.NO	Materials used (grams)		Total weight (grams)
	D-Mannitol	Graphene (%) (nanoparticle)	
1	10	0	10
2	9.75	0.25	10
3	9.50	0.50	10
4	9.25	0.75	10
5	9.00	1.00	10

3. Degradation Kinetic Analysis of Nano PCM

In thermal analysis, activation energy and other kinetic parameters are essential in order to understand degradation and reaction pathways of a given material. Iso-conversional methods such as the KAS (Kissinger-Akahira-Sunose), the FWO (Flynn-Wall-Ozawa), and the Starink methods are often utilized for these analyses without much knowledge of the reaction mechanism, thus allowing valuable information about activation energy and other parameters to be readily extracted and permitting the progression of materials and technologies. This section reviews the principles, methods, and uses of the three most relevant techniques for thermal analysis [29].

Heating rates of 10, 15, 20 and 25 °C min^{-1} were selected in accordance with ICTAC recommendations for non-isothermal kinetic analysis to produce accurate characterisation of the thermal degradation processes easy of the materials, free of thermal lag or instrument drift. Lower rates of heating of <10 °C min^{-1} tend to inhibit the time period for testing and lead to an instability in the baseline, while higher heating rates of 25 - 30 °C min^{-1}

give rise to non-uniform internal temperature gradients. The selected range thus provides a compromise between kinetic accuracy and practical thermal conditions. In addition, heating rates in this range are also similar to those in industrial applications of the PCMs, for example, solar thermal charging and discharging cycles and thermal management of electronic devices, where the temperature rise usually lies between 5 and 30 °C min^{-1}. The TGA rates used in this work therefore, are also realistic in terms of mimicking commercially useful operational conditions while ensuring reproducibility in the experiments.

3.1 KAS (Kissinger-Akahira-Sunose) Method

The Kissinger–Akahira–Sunose (KAS) approach is a commonly used isoconversional technique for analyzing non-isothermal degradation kinetics. The more recent refinements have rendered possible the extension of the classical Kissinger technique to multi-step degradation systems, which gives a greater accuracy to estimates of activation energy throughout complex paths or reaction routes [29].

$$ln\left(\frac{\beta}{T^2}\right) = ln\left(\frac{AR}{E_a}\right) - \left(\frac{E_a}{RT}\right) \quad (1)$$

The updated isoconversional formalism derived by Tarani *et al.* (2024) was adopted here to ensure accurate evaluation of activation energies in the multi-stage degradation of D-Mannitol and GNP-modified composites [30].

3.2 FWO (Flynn-Wall-Ozawa) Method

The FWO approach is an isoconversional method of calculating activation energy for thermal decomposition, based on integral concept that circumvents assumptions of a specific reaction mechanism and is usually a more flexible overall analysis [31].

$$ln(\beta) = ln\left(\frac{AE_a}{Rg(\alpha)}\right) - 2.315 - 0.4567\left(\frac{E_a}{RT}\right) \quad (2)$$

3.3 Starink Method

The Starink approach is an isoconversional method most similar to KAS and FWO methods, but takes a more straightforward approach to adjusting the KAS equation, offering a new perspective in the field of chemical reactions in general with more specific variables to effectively analyze reaction kinetics and activation energy [32, 33].

$$log\left(\frac{\beta}{T_\alpha^{1.92}}\right) = \text{constant} - \frac{1.008E_a}{RT_\alpha} \quad (3)$$

The KAS, FWO, and Starink models were selected because they effectively analyze both isothermal and non-isothermal TGA data without assuming a specific reaction mechanism [6]. These model-free approaches estimate activation energy (E_a) as a function of conversion (α), providing a more reliable interpretation of multi-step degradation than single-step methods. While KAS and FWO balance computational simplicity with accuracy, the Starink model refines their logarithmic approximation to reduce systematic error [7]. Previous studies have shown their E_a values to agree within ±5%, confirming their suitability for evaluating the thermal stability of nano-enhanced materials [8, 9].

3.4 Machine Learning Models

Regression Analysis is primarily a statistical technique used to predict and understand the relationship between different variables through machine learning. There are several regression methods available (e.g., Linear Regression, Polynomial Regression, Random Forest Regression) with various algorithms that can be used to model the relationships in unique ways. Each type of regression also has its own specific application or use case for different types of data and context based problem solving.

3.5 Validation for ML models and uncertainty

All models were evaluated through five-fold cross-validation (K=5), and their predictive performance was assessed using statistical indicators such as R^2, RMSE, and MAE [14]. To estimate predictive uncertainty in the models, Quantile Regression Forests were utilized to estimate 95% prediction intervals [18]. Coverage (PICP) and average interval width were estimated to assess calibration, methods, and the basis of each application to problems, and possible disadvantages [19].

3.5.1 Linear regression

In machine learning, linear regression establishes a linear relationship between the dependent variable y and one or more independent variables X using the equation [8-19].

$$y = \beta_0 + \beta_1 X + cY \quad (4)$$

Where β_0 represents the intercept, β_1 denotes the slope, and ϵ is the error term. The parametersβ_0 and β_1 are obtained by applying the least squares method, which minimizes the total squared differences between predicted and actual values. For cases involving multiple predictors, this formulation extends to a multivariable linear regression model.

$$y = \beta_0 + \beta_1 X + \beta_2 X_2 + \cdots\cdots + \beta_P X_P \varepsilon \quad (5)$$

While linear regression is simple and effective, it may not capture complex patterns, for which polynomial regression is often employed.

3.5.2 Polynomial Regression

Polynomial regression represents the relationship between the independent variable x and the

dependent variable y using an n^{th} -degree polynomial equation, enabling the model to capture nonlinear trends that simple linear regression cannot. The general expression is given as:

$$\beta_0 + \beta_1 x + \beta_2 x^2 + \beta_3 x^3 + \cdots \ldots \ldots . + \beta_n x^n + \in \quad (6)$$

3.5.3 Random Forest Regression Analysis

Random Forest Regression uses the combination (or aggregation) of multiple decision trees to generate predicted values for a continuous outcome variable. Each decision tree is created based upon a randomly selected subset of the training dataset. With this approach, the issue of overfitting is reduced when compared with using a single decision tree. The process in which a decision tree splits at each node includes the selection of a random subset of predictor variables. As such, each tree is unique. The final value of the function f(x), representing the predicted value of the model for input x, is determined as the average of the output values generated by each of the T trees.

$$f(x) = \frac{1}{T}\sum_{i=1}^{T} f_i(x) \quad (5)$$

To ensure transparency and robust predictive performance, hyperparameter tuning was conducted using the grid-search method, examining the following parameters: the number of trees (50–500), the maximum depth (5–20), and the minimum sample split (2–5). A 10-fold cross-validation technique was conducted for assessment of model stability and avoidance of overfitting. The data were randomly partitioned into 80% training and 20% testing. The feature-importance ranking indicated temperature and heating rate to be the principal predictors governing the mass-loss behaviour. This tuning process and interpretability analysis ensured that the Random Forest model was not only accurate but also generalizable.

4. Results and Discussions

4.1 Thermogravimetric Analysis

Thermal degradation behaviours of Pure D-mannitol and its GNP composite were evaluated by TGA at four heating rates of 10, 15, 20 and 25 °C·min⁻¹. The total weight loss – temperature relations for all samples are shown in Figure 3(a–e). As seen from Figure 3(a), it is demonstrated that Pure D-Mannitol exhibits a high level of thermal stability until about 350 °C. There is no weight loss for Pure D-Mannitol up to this temperature [7, 8].

Decomposition begins as early as 350°C-400°C; as the heating rate is increased, the onset of decomposition increases from approximately 360°C (at 10°C·min⁻¹) to around 390°C (at 25°C·min⁻¹). A significant decline in mass loss occurs from 380°C to 450°C, when all components of the D-Mannitol are decomposed. These observations suggest that D-Mannitol undergoes one predominant decomposition mechanism, which is primarily influenced by the crystalline to amorphous phase transition followed by fragmentation of molecules [9-12].

The thermal degradation profiles for samples of D-Manitol reinforced with GNPs at concentrations of 0.25 wt% and 0.50 wt%, were virtually indistinguishable from the D-Manitol thermal degradation profile alone (see Figs 3b and c). As shown in Figs 3b and c, the initial degradation temperature (T-onset) and the slope of the mass loss versus time plot (i.e., a measure of the rate of thermal degradation) for the composite samples were very close to those measured for the neat PCM; suggesting that low levels of filler loading did not appreciably degrade the bulk thermal stability of the PCM. Thus, at these relatively low filler loadings, it appears that GNPs primarily serve as thermally conductive fillers which do not substantially modify the chemical kinetics of the material's thermal decomposition [27].

The TGA profiles show a difference at the higher filler loadings (0.75 wt% and 1 wt%) relative to the TGA profiles of D-Mannitol alone. In figures 3(d) & 3(e), the temperature of the beginning of degradation is slightly higher for each composite compared to D-Mannitol alone. This represents a slight increase in thermal stability. This could be attributed to the GNPs acting as thermal barriers and stabilizers, limiting the transfer of heat and causing a delay in the decomposition of D-Mannitol. However, the overall shape of the TGA curves does not vary significantly, which indicates that the degradation process for all of the composites is single-step processes [3-6].

4.2 Multi-Step Degradation Behaviour

The TGA plots of both pure and GNP-Doped D-Mannitol show a two-step degradation process, as can be seen by comparing the TGA traces shown in Figure 3. The first phase (from approximately 50–150 °C) is due to the removal of surface water and weakly bonded volatile compounds and accounts for less than 3% total weight loss. The second and most significant phase (from approximately 350–480 °C) represents thermal decomposition of D-Mannitol via cleaving C–O and C–C bonds to create major weight losses and volatile products. The GNPs have elevated the temperature at which D-Mannitol begins to decompose; therefore, they are acting as heat transfer agents and barriers to volatile product diffusion and are thus enhancing the thermal stability of D-Mannitol. Additionally, the kinetic analysis using the KAS, FWO and Starink models has demonstrated a two-phase behaviour for each sample set with lower E_a for the initial step and higher E_a for the main degradation region, indicating the multi-step kinetics of the composite system.

4.3 Residual Mass Analysis

The residual mass is mostly due to the thermally stable graphene nanoplatelet (GPN) portion, which retains its structure under the nitrogen atmosphere and acts as an inert and non-volatile reinforcing agent, hindering full mass loss, and secondarily to the carbonaceous char formed by pyrolysis of the organic phase.

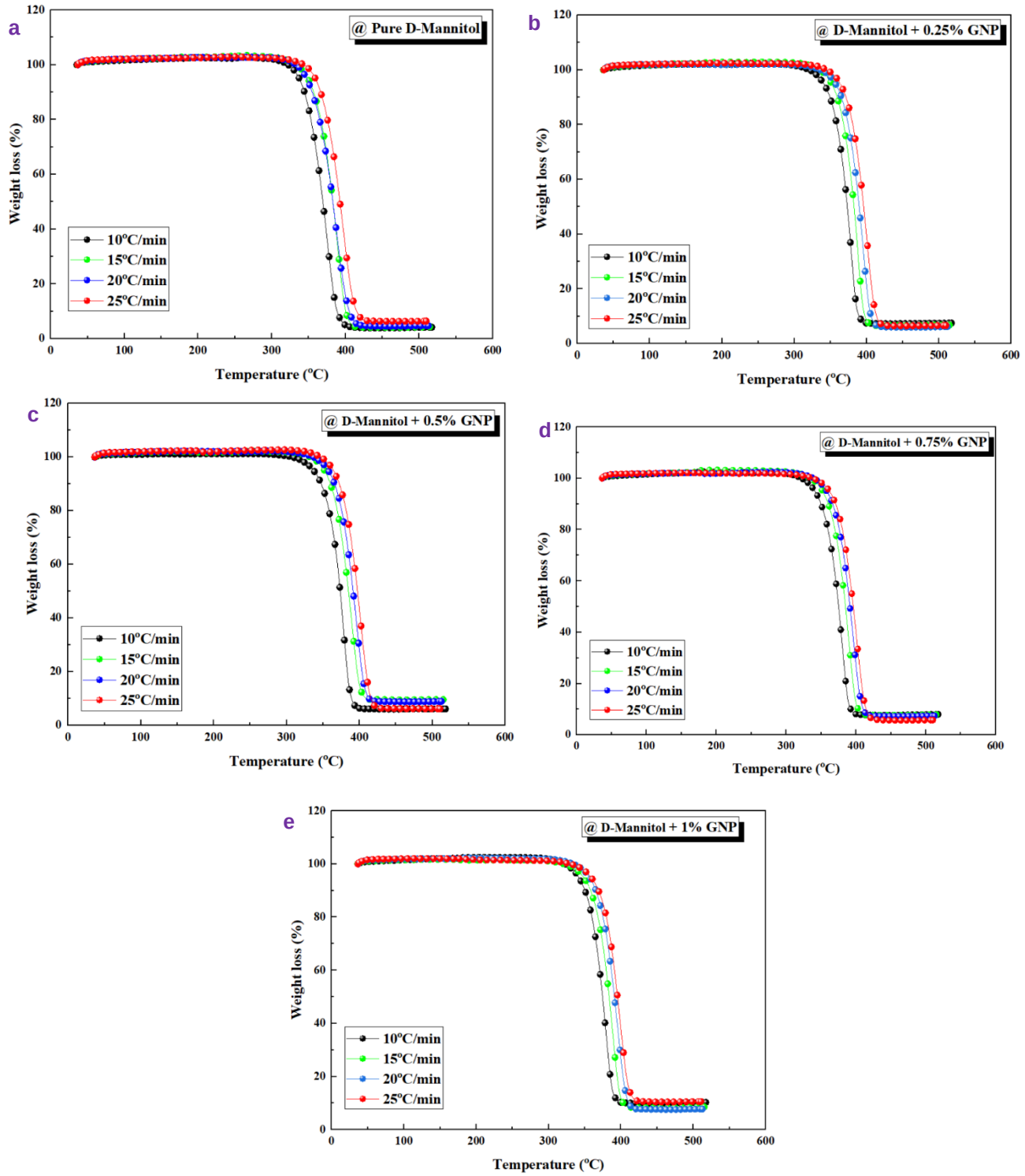

Figure 3(a). Thermogravimetric analysis (TGA) curve of pure D-Mannitol at different heating rates (10–25 °C min^{-1}), **(b).** Thermogravimetric analysis (TGA) curve of D-Mannitol containing 0.25 wt% graphene nanoplatelets (GNPs) at heating rates of 10–25 °C min^{-1}, **(c).** Thermogravimetric analysis (TGA) curve of D-Mannitol containing 0.5 wt% graphene nanoplatelets (GNPs) at heating rates of 10–25 °C min^{-1}, **(d)** Thermogravimetric analysis (TGA) curve of D-Mannitol containing 0.75 wt% graphene nanoplatelets (GNPs) at heating rates of 10–25 °C min^{-1}, **(e).** Thermogravimetric analysis (TGA) curve of D-Mannitol containing 1 wt% graphene nanoplatelets (GNPs) at heating rates of 10–25 °C min^{-1}.

Pure D-Mannitol demonstrates near complete volatilization with less than 1% remaining as residue, while for GNP-containing samples, the residual mass ranges between 1.5-4% depending on the filler content. The fact that there is a non-volatile component (residue) supports the observed improvement in thermal stability and indicates indirectly that the GNP's structure persists at high temperature.

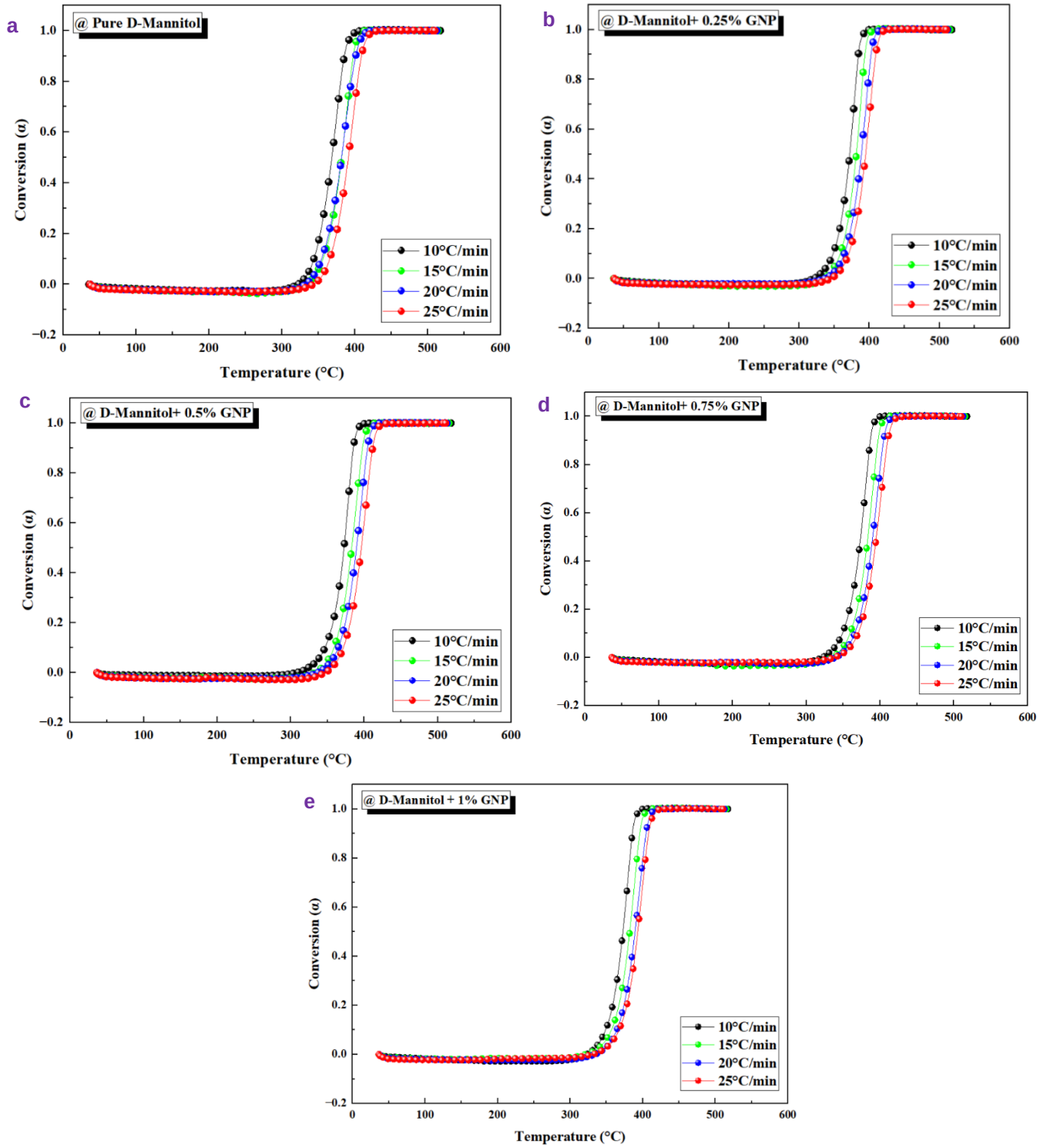

Figure 4(a). Conversion (α) vs. temperature (T) plot for pure D-Mannitol at heating rates of 10–25 °C min^{-1}, showing the onset and progression of thermal decomposition, **(b).** Figure 4(b). Conversion (α) versus temperature (T) for D-Mannitol with 0.25 wt% GNPs at heating rates of 10–25 °C min^{-1}, depicting the start and trend of thermal degradation. **(c).** Figure 4(b). Conversion (α) versus temperature (T) for D-Mannitol with 0.5 wt% GNPs at heating rates of 10–25 °C min^{-1}, depicting the start and trend of thermal degradation. **(d).** Figure 4(b). Conversion (α) versus temperature (T) for D-Mannitol with 0.75 wt% GNPs at heating rates of 10–25 °C min^{-1}, depicting the start and trend of thermal degradation. **(e).** Figure 4(b). Conversion (α) versus temperature (T) for D-Mannitol with 1.00 wt% GNPs at heating rates of 10–25 °C min^{-1}, depicting the start and trend of thermal degradation.

4.4 Estimation of conversion efficiency of D-Mannitol and GNP Composites

The conversion efficiency, α, is important in determining how phase-change materials (PCMs) degrade thermally, which also shows the thermal stability of PCMs. The conversion efficiency, α, was obtained by TGA to obtain the fraction of material that has been converted versus temperature (T), and heating rate (HR) [3, 6, 11].

The conversion efficiency will allow a comparison between the effect of Graphene Nanoplatelets (GNPs) on both thermal stability and kinetic behaviour of D-mannitol. The α-T curves for pure and composite samples were established at different heating rates (10, 15, 20, 25° °C min^{-1}) as seen in the Figure 4(a-e).

Similar to the previous Figure 4(a), pure D-Mannitol starts degrading around 350 °C and is mostly gone by 450 °C. At low heating rates (10 °C min^{-1} and 15 °C min^{-1}), the start of conversion occurs prior to those heating rates found at high heating rates (20 °C min^{-1} and 25 °C min^{-1}), which cause the α-T curves of the latter to be moved toward higher temperatures due to the effect of the heating rate on the kinetics of degradation. A low heating rate will produce a more even distribution of energy and, therefore, a faster initiation of decomposition.

The addition of 0.25 wt % GNP causes a slight shift in the temperature conversion curve of FIG. 4 (b) to greater temperature values, as depicted in Fig. 4(b). Therefore, GNP improves the thermal stability of the composite by uniformly distributing the heat generated in the matrix, thereby delaying the start of degradation and yet retaining the same mechanism of degradation for the matrix itself.

The conversion curves for the 0.5 wt% GNP composite illustrated in Fig. 4(c) display the same general thermal behaviour as those of the 0.25 wt% composite. Although the temperature of onset of decomposition is still located within the same temperature range (350 – 400 °C) it was observed that the delayed conversion at increased heating rates was indicative of a moderate increase in kinetic stability of the system. Thus, the kinetic enhancements observed at low GNP concentrations are largely due to the improved thermal conductivity of the composite materials rather than through interactions of a chemical nature.

In the case of GNP loadings at 0.75 wt %, a significant change in the position of the temperature-conversion profile is seen; as such this illustrates an increased thermal stability of the samples. A delay in the start of the degradation process is observed, with most of the conversion occurring over the 350 °C to 500 °C range. It can be inferred that improved interfacial contact between the GNPs and D-mannitol has resulted in improved uniformity of the absorbed energy and consequently decreased the thermal decomposition rate.

As shown in Figure 4 (e), the 1 wt% GNP composite has demonstrated the best thermal stability out of all composites investigated. Thermal decomposition for the composite begins at about 400°C and ends at about 500°C, showing an increase in thermal stability due to increased GNP concentration. The α-T profiles clearly demonstrate that GNP is a thermally stable reinforcing material which suppresses the volatilization and delays the degradative process. All composite systems are in the same conversion range however, there has been a clear trend toward higher decomposition temperature with increasing GNP content.

In this study, the word conversion applies solely to the thermal decomposition progress (α) taken from a TGA mass-loss route in nonisothermal conditions, being the part of the material that has undergone degradation in some form by thermally induced effects at a specific temperature and heating rate, not to denote any form of chemical or structural change. The forms of conversion reported in this work are therefore indicative of kinetic behaviour rather than chemical change or phase formation. No spectroscopic or microstructural work (FTIR, XRD and SEM) was undertaken in this study, but the close agreement of the KAS, FWO and Starink activation-energy methods of study supports the reproducibility of the thermal-conversion studies undertaken. Detailed FTIR and XRD studies will be undertaken in the future, aimed at establishing the integrity of D-mannitol in chemical form, and at studying the probability of GNP taking place during heating.

4.5 Activation-Energy Evaluation

Determining the activation energy (E_a) of phase-change materials (PCMs) is important to determine how PCMs decompose thermally and to establish what stabilization methods are effective for PCM decomposition processes. In this study, three of the most commonly utilized isoconversional kinetic models [Kissinger-Akahira-Sunose (KAS), Flynn-Wall-Ozawa (FWO), and Starink] were employed to compare the effect of adding Graphene Nanoplatelets (GNPs) to D-Mannitol as a method of improving its thermal stability.

The difference in values for activation energy calculated by Starink vs. those from KAS/FWO is due to that fact that Starink's calculated 61.99 kJ mol^{-1} relates to the initial conversion (i.e., $\alpha \approx 0.1$), while the larger values of ~130-150 kJ mol^{-1} are averaged over the major decomposition region ($\alpha \approx 0.3 – 0.8$). As indicated in Figures 5(a–e), the variation of activation energy with degree of conversion (α) for both pure and GNP-enriched composite samples are depicted [15]. The activation energy for pure D-Mannitol is depicted in figure 5 (a) as being approximately the same over all of the conversion range at around 130-140 kJ mol^{-}.

Figure 5(a). Variation of activation energy (E_a) with conversion for pure D-Mannitol determined using KAS, FWO, and Starink model-free approaches. **(b).** Activation energy (E_a) versus conversion for D-Mannitol with 0.25 wt% GNP, evaluated using the KAS, FWO, and Starink model-free methods. **(c).** Activation energy (E_a) versus conversion for D-Mannitol with 0.5 wt% GNP, evaluated using the KAS, FWO, and Starink model-free methods. **(d).** Activation energy (E_a) versus conversion for D-Mannitol with 0.75 wt% GNP, evaluated using the KAS, FWO, and Starink model-free methods. **(e).** Activation energy (E_a) versus conversion for D-Mannitol with 1.00 wt% GNP, evaluated using the KAS, FWO, and Starink model-free methods.

KAS method shows the most consistent data of the three methods, therefore, it has the highest level of accuracy and reliability. The activation energy profile is relatively flat indicating that there is a single step degradation mechanism occurring due to molecular chain scission [27]. At 0.25 wt % GNP (Figure 5(b)), the activation-energy stability slightly increases as the conversion is increased along with very minimal difference among the different models. The values from Ozawa are ever so slightly larger than those obtained through KAS, while those from Starink are still intermediate. Thus, it can be inferred that an additional 0.25 wt % of GNP will improve the energy barrier to decomposition for thermal degradation which will result in improved thermal stability and will not alter the degradation mechanisms.

At a 0.5 wt% GNP loading, the activation energy plots displayed in figure 5(c) are also consistently observed for all conversion levels. KAS is still displaying the lowest Ea (≈ 130–140 kJ/mol) values, while both FWO and Starink have slightly higher Ea values that are parallel to one another. Thus, it appears that adding an intermediate amount of GNP results in kinetic stabilization that balances the loss of thermal conductivity due to GNP while maintaining the structural integrity of the matrix.

At a weight percentage of 0.75 wt% GNP, it can be observed from Figure 5(d) that an increased activation energy with values ranging about 140 – 150 kJ/mol. These values indicate that there exists a stronger interfacial interaction between the GNPs and D-Mannitol; as such, molecular mobility is restricted and the energy needed to decompose will be higher. Additionally, the close agreement among the three models shows that this stabilizing effect is physically consistent.

GNP composites have the largest E_a values for 1 wt% GNP composites, as illustrated in Fig. 5(e), which is consistent with GNPs acting as reinforcement. The three model-free methods show similar trends with very small changes throughout the conversion range. It can be concluded that above a certain loading level, GNPs act to reduce heat transfer by forming a barrier layer to the thermal degradation process and therefore increase the required activation energy.

4.6 Statistical Evaluation of Activation-Energy

Statistical evaluation of the differences among the kinetic models and GNP loadings at different conversion levels (α) was conducted via analysis of the trend of activation energy (Ea) as a function of conversion level (α). For each α value, plots of Ea(α) versus β (heating rate) were made using a 95% bootstrap confidence interval (CI) for Ea(α) values for each β value. The statistical comparisons of differences among kinetic models (KAS, FWO, Starink) and GNP loading concentrations were made using an ANOVA, followed by Holm corrected pair-wise t-tests ($p < 0.05$). The above mentioned statistical measures provided statistical confidence in the observed trends of activation energy for each α. The average ± standard deviation (SD) of activation energies determined from the three non-isothermal kinetics methods for all concentrations of GNP are shown in Table 6, which demonstrates a progressively increasing trend of Ea with increasing concentrations of GNP, providing evidence that the addition of nanomaterials enhances the thermal stability of the composites.

4.6.1 Effect of GNP on Activation Energy Trends

Variations in activation energy (Ea) as a function of conversion fraction (α) indicate that GNP influence is differently exerted at different decomposition stages. For α 0.5, Ea steeply increases, implying that GNPs are acting as barrier materials that hinder mass transfer and volatile release. The thermal conductivity provided by an interconnected GNP network allows for uniform temperature distribution and enhanced interfacial phonon transport, resulting in higher energies being needed to continue degradation. The variation of Ea indicates that there is a transition from surface initiated reactions to stabilization of the bulk PCM matrix. Other researchers have identified similar dual behaviours for both CNT and GNP enhanced PCMs [2 - 4, 7].

4.6.2 Statistical Evaluation of Activation-Energy

A One-Way Analysis of Variance (ANOVA) was performed to provide a quantitative evaluation for whether the observed differences in activation energy (E_a) were statistically different at each of the three kinetic models (KAS, FWO and Starink) and across each of the various GNP loadings (0-1 wt%) as follows: E_a versus wt% GNP concentration was shown to be highly statistically significant ($F= 16.84$, $p = .012$ .05); thus, the KAS, FWO and Starink methods produce similar activation energy (Ea) values.

Further, subsequent pairwise t-tests using Holm correction indicated that the 0.75 wt% and 1 wt% GNP composite materials exhibited significantly higher activation energies ($p < .05$) than the pure PCM, whereas the 0.25 wt% and 0.5 wt% GNP composite materials did not exhibit statistically significant differences. Thus, the statistical results provided by the t-tests demonstrate that additions of GNP greater than 0.5 wt% contribute to an actual and measurable enhancement in thermal stability, validating both the stabilizing effect of GNP and the reliability of the kinetic models used.

Our calculated E_a-values for D-Mannitol + GNP (about 130–149 kJ mol^{-1}) match very closely with the ones found for CNT-enhanced paraffin PCMs [3] and graphene-modified fatty-acid PCMs [4, 6]. The latter have a range from 120 to 155 kJ mol^{-1}.

Table 6. Activation-energy (Ea) values for pure and GNP-enhanced D-Mannitol obtained from KAS, FWO, and Starink model-free methods

GNP (wt %)	KAS (kJ mol^{-1})	FWO (kJ mol^{-1})	Starink (kJ mol^{-1})	Mean ± SD (kJ mol^{-1})
0	137.62	141.48	61.99	113.70 ± 43.4
0.25	123.67	149.08	119.33	130.69 ± 15.9
0.50	130.00	138.00	140.00	136.00 ± 5.3
0.75	145.00	147.00	142.00	144.67 ± 2.5
1.00	146.00	149.10	145.80	146.97 ± 1.7

Table 7. Effect of Temperature on D-Mannitol–GNP Samples at Various Heating Rates

Sample Type	**10^0 C min^{-1}**	**15^0 C min^{-1}**	**20^0 C min^{-1}**	**25^0 C min^{-1}**
Pure Mannitol	300.8	306.7	308.7	321.3
0.25% GNP	307.9	311	320.6	330.5
0.5% GNP	304.7	314	321.4	351
0.75% GNP	308.8	319.6	327.7	335.4
1 % GNP	310.5	321.3	328.4	335.8

The similarity with these data confirms that our experimental model-free and machine learning based results are accurate and consistent with previous findings. E_a values for D-mannitol + GNP (≈ 130-149 kJ·mol^{-1}) found in this study are comparable to those of other open access studies of nano-enhanced organic PCMs. Kottala *et al.* (2023), as an example, report average E_a values of ~65-86 kJ·mol^{-1} for pure sugar-alcohol PCM and ~52-79 kJ·mol^{-1} when 0.5–1 wt% MWCNT are added [7]. Said *et al*. (2024) also provide a comprehensive review stating that graphene- or CNT-based fillers have been shown to increase both the thermal stability and E_a threshold across many PCM systems [2]. The comparison of these results supports the same trend seen in this study and further validates the increased thermal stability provided through GNP addition.

4.6.3 Comparison of Kinetic Models

The three methods of evaluating kinetic models used in this study (Starink, KAS and FWO) indicated that Starink was the most consistent and effective activation energy (Ea) estimator throughout the loading levels of GNP (Graphene Nanoplatelets) and conversions of D-Mannitol–GNP composite samples (α = 0.1 – 0.9). The correlation coefficients for the linear relationships obtained from $\ln(\beta/T^2)$ vs 1/T for the Starink method were greater than R^2 = 0.99, and Ea variations using the Starink method were within ±2.5 kJ mol^{-1}, showing a relatively stable response. Activation energies estimated by the KAS method had slightly larger variations (±5.3 kJ mol^{-1}) as a result of the sensitivity of this method to changes in heating rate. The FWO method consistently predicted higher Ea values for conversions above α = 0.7, resulting from the errors associated with approximations in integration. Based on these results, it is evident that the Starink method was the most robust non-isothermal kinetic model evaluation technique for analyzing D-Mannitol-GNP composite materials and provides an excellent balance of ease of calculation with high prediction accuracy.

4.6.4 The Impact of Temperature and Graphene Nanoparticles on the Thermal Properties of Mannitol

By examining the changes in a specific measured property (such as melting point, thermal conductivity, or solubility) at different temperatures, we aim to understand how the addition of GNP influences the thermal or physical properties of mannitol.

Table-7 provides a useful representation of pure mannitol and mannitol with 0.25%, 0.5%, 0.75%, and 1% GNP, all at temperatures between 10°C min^{-1} and 25°C min^{-1}. These data substantiate the purported enhanced effect of GNP on mannitol and provide useful evidence in support of the development of mannitol-GNP composites for a variety of temperature sensitive applications.

4.7 Machine Learning Prediction Results

The use of machine learning (ML) was used to model how the thermal degradation of D-Mannitol and its Graphene-Nanoplatelet (GNP) composite material would occur with varying temperatures [12].

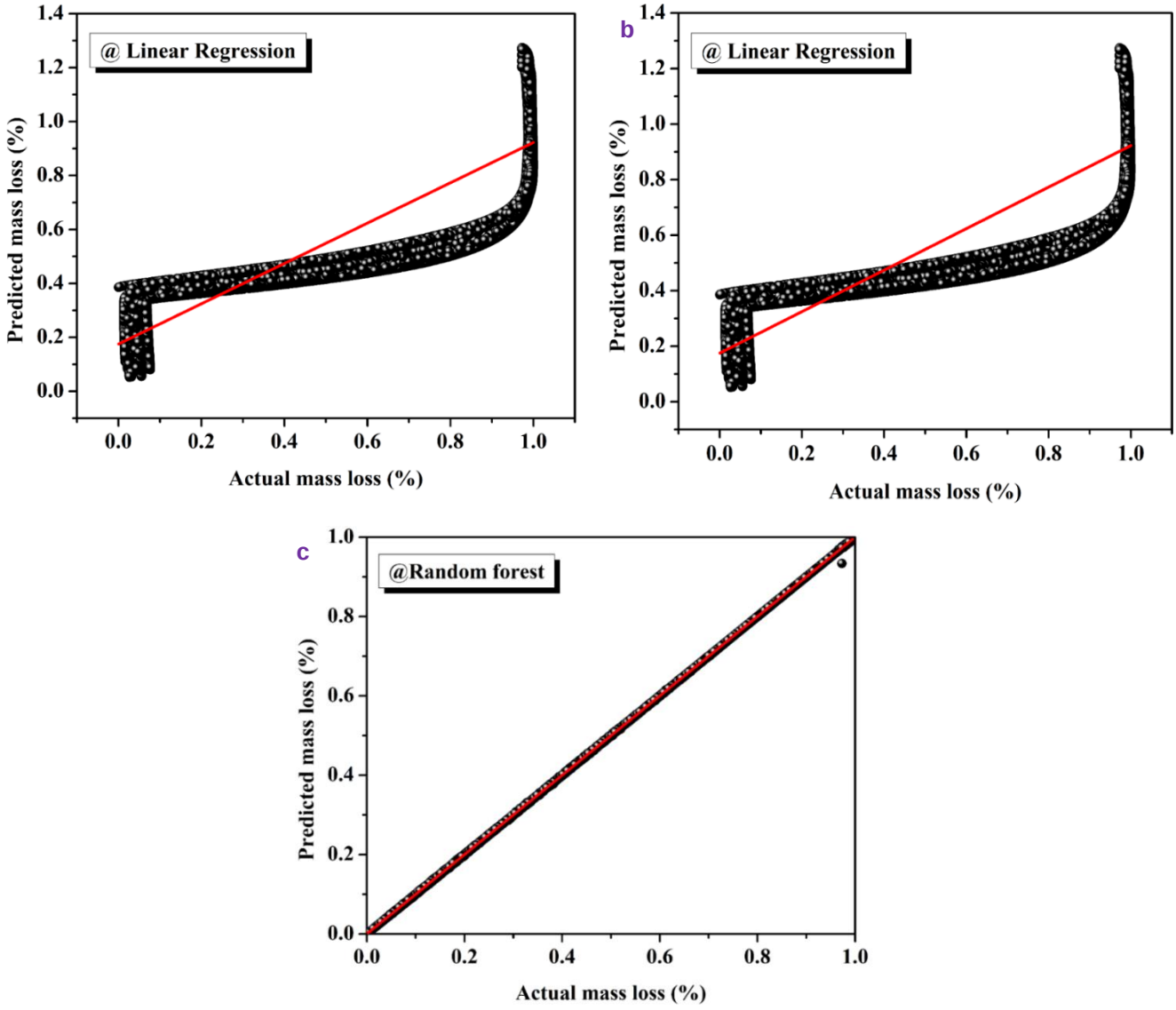

Figure 6(a). Comparison of actual and predicted mass-loss percentage using the linear regression model. **(b).** Comparison of actual and predicted mass-loss percentage using the polynomial regression model, showing improved fit for nonlinear data. **(c).** Comparison of actual and predicted mass-loss percentage using the random forest regression model, demonstrating superior prediction accuracy

In addition to kinetic analysis, three machine learning models (linear regression, polynomial regression, random forest regression) were compared using experimental TGA data to determine their ability to accurately model mass loss behaviours from those experiments [13]. Each of the three machine learning models' ability to model mass loss behaviours was determined using figures that show the percentage of mass loss between the experimentally measured data versus the modelled predictions (figures 6a-c).

The linear regression model depicted in figure 6 (a) successfully captured the downward trend of mass loss with increased temperature, as shown in the figure. However, its limited accuracy is apparent at mid to higher temperatures where the degradation of PCM's by heat follows non-linear processes. Thus, these are examples of the limitations of using a purely linear relationship to describe the complex process of thermodecompositon of PCM's modified with GNP [14].

A polynomial regression model is applied to provide a more accurate representation of the nonlinear relationships between temperature and mass loss rates. Polynomial models (as shown in Figure 6b) demonstrate superior fitting when compared to linear models, especially where the rate of mass change increases rapidly. Higher order terms allow the model to capture non-linear behaviour (curvature of the data), thus allowing the model to predict the degradation phase [21] more accurately.

Random Forest Regression (RF) was the most effective model overall due to being an Ensemble Learning Technique using Multiple Decision Trees to make a prediction. In Figure 6(c), the Predicted Mass-Loss Profile is nearly identical to the Experimental Data at all Temperature Ranges, indicating that the Random

Forest Model has good Generalization Capability and Low Deviation. Overall, the Random Forest Model captured both Linear and Non-Linear Dependencies between Thermodegradation Kinetics and Temperature far better than the Linear and Polynomial Models, which indicates that it is well-suited to model the Complex Thermodegradation Kinetics of Nano-Enhanced PCMs [22].

The reason that the random-forest-regression model provides a better prediction is that it can find non-linear interactions between variables (heating-rate, temperature, and GNP) in addition to the hierarchical dependencies between the variable inputs. The random-forest-regression model does this by using an ensemble of multiple decision-trees to predict the relationship between the input variable(s), rather than relying on a single decision tree as with linear or polynomial regression models. In contrast to using a single decision-tree as with linear or polynomial regression models, which assume that there are either fixed or specific relationships between input variables and the output variable(s); the use of decision-trees within an ensemble approach results in a reduction in over-fitting, while maintaining the ability of the model to generalize; therefore explaining the near perfect correlation between the predicted and experimental mass loss data.

Among the many models tested, random forest regression was most successful in achieving prediction accuracy with an R^2 = .99 and RMSE of 0.0002, which validates the power of this ensemble method to correlate TGA derived data [26] accurately. This shows that ensemble methods using machine learning (ML) can be successfully used to predict trends from thermal degradation and therefore, could potentially be used as a reliable tool for predicting the stability of phase change materials (PCMs) and help to optimize designs for energy storage systems.

4.8 Dataset and Reproducibility Details

A dataset was created to be utilized as input into the machine learning models through thermogravimetric analysis (TGA) that was run on 5 different composite formulations of D-Mannitol-GNP (0% GNPs, 0.25% GNPs, 0.5% GNPs, 0.75% GNPs and 1% GNPs) at four heating rates (10, 15, 20 and 25 °C min−1). The TGA data produced mass loss data for each sample at 24 temperatures, which ultimately resulted in 480 data points. The input features were temperature (°C), heating rate (β), and wt% GNP; the output feature was wt% mass loss. All features were normalized prior to model training by utilizing Min-Max scaling to be bounded by 0-1. For all three types of models, 80% of the data was used for model training and 20% was used for model validation; this process was repeated ten times with a new random subset of data selected each time to help prevent model overfitting.

4.9 Mechanistic understanding, constraints and uncertainties

Mechanism: A network of highly conductive graphene nanoplatelets (GNP), dispersing the heat generated and reducing localized hotspot formation, improved interface phonon transmission and platelet barrier effect reduces volatile diffusional pathways and delays scission/evaporation processes and thus moves the temperature of mass loss onset to higher temperatures. The extent of this stabilization is dependent upon the GNP's aspect ratio, the average platelet size and uniformity of dispersion of the GNPs, affecting the percolation threshold and thermal boundary conductance.

Limitations and generality: Degradation routes in sugar-alcohol matrixes (D-mannitol) differ from those of paraffin matrixes; therefore, confirmation of the trends identified here must occur in each type of matrix separately prior to generality being established. Also, the results of this work may depend on the degree of uniformity of nanofiller dispersion, the thickness of the samples and the range of β used in TGA; these have been cited as a limitation of this work.

Quantifying uncertainty: The kinetic $E_a(\alpha)$ values are reported with 95% confidence intervals determined via the bootstrap method at multiple heating rates (B = 200). Machine learning predictions include 95% prediction intervals based on Quantile Regression Forests for calibrating uncertainty in the predicted mass loss. Both the kinetic and machine learning results provide quantitative measure of the confidence in both types of analysis. These quantified uncertainties reinforce the reliability of both the kinetic and machine-learning analyses for use in industrial PCM design workflows.

All of the models' prediction reliability was assessed through the use of 10 fold cross validation and a summary of each of the models' statistical performance is found in table 6. The random forest regression model had the most accurate predictions with the highest r-squared value at .999999 and lowest root mean squared error of .000311, demonstrating nearly perfect correlation to the mass loss measured for each sample. The polynomial regression model also demonstrated high accuracy as it had the second-highest r-squared value (.9957) and second-lowest root mean squared error (.0262). The linear regression model had the least amount of prediction accuracy (.7478 r-squared and .2000 root mean squared error).

Table 8. Model Performance Metrics

Model	R^2	RMSE
Linear Regression	0.7478	0.2000
Polynomial Regression	0.9957	0.0262
Random Forest Regression	**0.999999**	**0.000311**

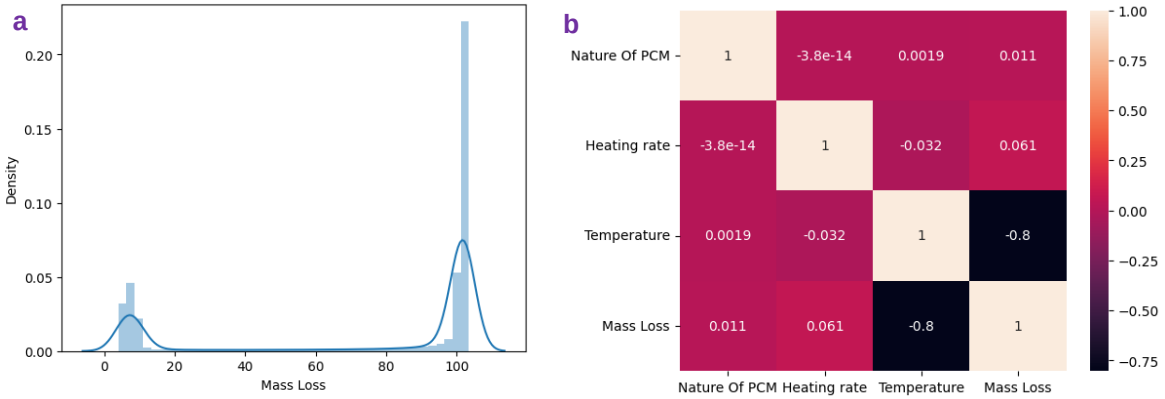

Figure 7(a). Mass-loss density distribution highlighting initial and final degradation regions, **(b)** Feature-correlation heatmap showing strong negative correlation between temperature and residual mass.

These findings show that non-linear and ensemble machine learning techniques can effectively determine the multi-variable degradation trends of nano enhanced phase-change materials systems and therefore provide model stability and reduce the likelihood of overfitting.

The predictive performance of all models were additionally analyzed through examination of correlations among features and distributions in the data. A density distribution plot (Figure 7(a)), shows a bi-modal distribution of mass loss data corresponding to the beginning and end of the degradation process. In addition, the correlation heat map (Figure 7(b)) illustrates a very strong negative correlation (r = –0.8) between temperature and residual mass indicating that temperature has been the primary factor influencing decomposition as observed from kinetic studies. Fig's 6(a-c), show the actual vs predicted mass loss behavior for the three regression models where Random Forest is nearly perfectly aligned and exhibits minimal scatter.

Therefore, together, the density distribution plots and correlation heat maps confirm that the Random Forest model is both interpretable and generalizable and demonstrates a high degree of correspondence between machine learning predictions and physical degradation mechanisms.

4.10 Application Implications

GNP modified D-mannitol exhibits improved thermal stability and oxidation resistance, which are critical for reliable, long-term performance in Thermal Energy Storage (TES) devices due to its enhanced activation energy (Ea) and altered mass loss characteristics. Improved thermal stability and oxidation resistance will translate to longer life cycles, less degradation and a more constant heat transfer coefficient over time in numerous applications including solar thermal collectors, building integrated PCM modules and waste-heat recovery systems. Higher activation energies of 130 – 149 kJ mol^{-1} were measured by the KAS, FWO and Starink models. These values imply greater energy requirements for decomposition of the composite which will lead to lower rates of degradation and increased chemical stability when subjected to repeat thermal cycling. Both attributes are important to achieving long term operational stability of TES modules.

The resultant increased safety and reliability of energy storage at medium temperatures provides additional advantages. Additionally, the success of employing machine learning (ML) models has allowed for the rapid assessment of degradation trends that could be utilized for real-time control and predictive maintenance in industrial TES applications. Thus, this research not only provides evidence of material level improvements, but it also supports a data-driven approach to design for future generations of PCM-based energy systems.

An increase in the activation energy (Ea) and decomposition temperature, which is an observable consequence of adding GNP to D-mannitol, results in increased operational safety and longer term operationally stable use of thermal energy storage (TES) and solar-thermal systems. Materials that have a larger activation energy value can be thermally degraded at a lower rate than materials that have smaller activation energy values; therefore, these materials are able to provide more consistent operation and chemical integrity across a wider range of temperatures before degrading. The ability to maintain stable operation and minimize the performance degradation after each cycle of charging and discharging enables the use of GNP-enhanced D-mannitol in TES systems for extended periods of time while maintaining high levels of system efficiency. Additionally, the increased decomposition temperature increases the upper operating temperature limit for the PCM; thus, it can be used effectively for medium-temperature solar-thermal applications, including concentrated solar power (CSP) collector systems and building integrated heat storage systems.

The D-Mannitol composites reinforced with GNP's have better activation energy gain and thermal cycle stability than other nano-enhanced PCMs

described in previous literature studies of nano-enhanced PCMs (CNT modified Paraffin [3]; Graphene-Oxide Based Fatty Acid PCMs [4, 6]). The enhanced performance is due to the high aspect ratios of GNP's and the ability to transfer phonons efficiently. Therefore, GNP's can provide enhanced performance compared to the spherical or amorphous nanofillers studied previously.

5. Conclusions

This study comprehensively evaluated the chemical and thermal stability, degradation kinetics, and predictive modelling of pure D-Mannitol and its graphene nanoplatelet (GNP) composites for medium-temperature thermal-energy-storage applications. Chemical stability improvements of the composites were demonstrated by thermogravimetric analysis (TGA), where it was shown that the total mass loss of the composites decreased significantly, from 98.6% for pure D-Mannitol to 95.4% for a composite with 1wt% GNP content. This decrease is attributed to the formation of a thermally stable carbonaceous residue and the reduction of volatile gas evolution from the material during pyrolysis. These results indicate that GNP acts as a chemically inactive thermal stabilizer that forms diffusion barriers to reduce oxidation and degradation of the D-Mannitol. In addition, the enhancement of thermal stability of the composites was confirmed by the increase in the activation energy (Ea) values of the composites determined using three model-free kinetic models — Kissinger-Akahira-Sunose (KAS), Flynn-Wall-Ozawa (FWO), and Starink — relative to pure D-Mannitol. In the case of pure D-Mannitol, Ea values ranged from 61.99kJ/mol (Starink) to 141.48kJ/mol (FWO). On the other hand, when GNPs are incorporated into D-Mannitol (i.e., 0.25-1 wt%), Ea values are found to range between 123.67kJ/mol and 149.08kJ/mol, which indicates an enhanced decomposition resistance and kinetic stability of the composites. A comparison of the three models indicated that the Starink method exhibited the most consistent trends over a wide range of heating rates, thereby validating its suitability for assessing the thermal stability of PCMs. Finally, machine learning (ML) analysis provided additional information about the mass loss behaviour of D-Mannitol and GNP composite samples. Specifically, a random forest regression (RF) model exhibited the highest prediction accuracy (R^2=0.99; RMSE=0.0002) relative to linear and polynomial regression models. Therefore, the use of RF and other ensemble-based machine learning algorithms may provide valuable tools for accurately predicting the performance characteristics of PCMs based on their thermo-kinetic properties.

6. Future work

The researchers suggest that future studies extend their approach to higher GNP loadings (1-3 weight %) and to other types of nano fillers, including carbon nanotubes (CNTs), Al_2O_3 and MXene sheets, to determine how the type of filler affects the kinetics. The researchers also suggest morphological and interface analysis (i.e., SEM, TEM, FTIR) to develop a relationship between structural characteristics and properties. Finally, the authors suggest using an explainable artificial intelligence (XAI) tool (i.e., SHAP or LIME) in conjunction with random forests to quantify uncertainties and to enhance interpretability. Additionally, the researchers suggest applying the hybrid kinetic-Machine Learning (ML) model to industrial energy storage devices via real-time PCM control systems and Bayesian optimization to create smart temperature management systems.

6.1. Key Implications

Stable chemical properties: The GNP increases the overall mass loss of materials, and limits volatile compound generation, to improve their chemical durability.

High thermal durability: Higher activation energies, and a longer time for decomposition indicate a higher temperature resistance for these materials.

Reliability with energy performance: The stable performance characteristics support reliable, long-term use of this technology at moderate temperatures.

Predictive ability of ML models: The random-forest model has been shown to predict degradation and stabilization patterns accurately.

Potential application as a practical technology: GNP-D-Mannitol PCMs have considerable potential to be applied in low-cost solar thermal and waste-heat recovery technologies.

6.2 Limitations

The current research is limited in that it only considered a maximum of 1 wt.% GNP. Therefore, the study did not assess the experimental effects of micro-structural distribution or the interface bonding of GNP. Based upon D-Mannitol as the base PCM the model can be generalized for use with other PCM types (i.e. paraffin or salt hydrate) through calibration. Additionally, the effect of uncertainty in repeatability of the experiments has not been evaluated and could potentially affect the variability of the fine-scale E_a values.

References

[1] L.E.A. Wijkhuijs, P. Schmit, I. Schreur-Piet, H. Huinink, R. Tuinier, H. Friedrich, Graphene nanoplatelet distribution governs thermal conductivity and stability of Paraffin-Based PCMs. Nanomaterials, 15(8), (2025) 587. https://doi.org/10.3390/nano15080587

[2] Z. Said, A. Pandey, A.K. Tiwari, B. Kalidasan, F. Jamil, A.K. Thakur, V. Tyagi, A. Sarı, H.M. Ali, Nano-enhanced phase change materials: Fundamentals and applications. Progress in Energy and Combustion Science, 104, (2024) 101162. https://doi.org/10.1016/j.pecs.2024.101162

[3] L. Yang, N. Zhang, Y. Yuan, X. Cao, B. Xiang, Thermal performance of stearic acid/carbon nanotube composite phase change materials for energy storage prepared by ball milling. International Journal of Energy Research, 43(12), (2018) 6327–6336. https://doi.org/10.1002/er.4352

[4] A. Shama, A.E. Kabeel, B.M. Moharram, H.F. Abosheiasha, Improvement of the thermal properties of paraffin wax using high conductive nanomaterial to appropriate the solar thermal applications. Applied Nanoscience, 11(7), (2021) 2033–2042. https://doi.org/10.1007/s13204-021-01903-7

[5] M. Aqib, A. Hussain, H.M. Ali, A. Naseer, F. Jamil, Experimental case studies of the effect of Al2O3 and MWCNTs nanoparticles on heating and cooling of PCM. Case Studies in Thermal Engineering, 22, (2020) 100753. https://doi.org/10.1016/j.csite.2020.100753

[6] L. Zhang, P. Zhang, F. Wang, M. Kang, R. Li, Y. Mou, Y. Huang, Phase change materials based on polyethylene glycol supported by graphene-based mesoporous silica sheets. Applied Thermal Engineering, 101, (2016) 217–223. https://doi.org/10.1016/j.applthermaleng.2016.02.120

[7] R.K. Kottala, B.K. Chigilipalli, S. Mukuloth, R. Shanmugam, V.C. Kantumuchu, S.B. Ainapurapu, M. Cheepu, Thermal degradation studies and machine learning modelling of Nano-Enhanced Sugar Alcohol-Based phase change materials for medium temperature applications. Energies, 16(5), (2023) 2187. https://doi.org/10.3390/en16052187

[8] L. Sun, Y. Qu, S. Li, Co-microencapsulate of ammonium polyphosphate and pentaerythritol and kinetics of its thermal degradation. Polymer Degradation and Stability, 97(3) (2011) 404–409. https://doi.org/10.1016/j.polymdegradstab.2011.12.003

[9] A.J. Otaru, Kinetics study of the thermal decomposition of date seed powder/HDPE plastic blends. Bioresource Technology Reports, 29, (2025) 102028. https://doi.org/10.1016/j.biteb.2025.102028

[10] K.P. Venkitaraj, S. Suresh, Experimental thermal degradation analysis of pentaerythritol with alumina nano additives for thermal energy storage application. Journal of Energy Storage, 22, (2019) 8–16. https://doi.org/10.1016/j.est.2019.01.017

[11] L. Xiang, D. Luo, J. Yang, X. Sun, Y. Qi, S. Qin, Preparation and Comparison of Properties of Three Phase Change Energy Storage Materials with Hollow Fiber Membrane as the Supporting Carrier. Polymers, 11(8), (2019) 1343. https://doi.org/10.3390/polym11081343

[12] T. Ahmad, H. Chen, Y. Guo, J. Wang, A comprehensive overview on the data driven and large scale based approaches for forecasting of building energy demand: A review. Energy and Buildings, 165, (2018) 301–320. https://doi.org/10.1016/j.enbuild.2018.01.017

[13] D.K. Bhamare, P. Saikia, M.K. Rathod, D. Rakshit, J. Banerjee, A machine learning and deep learning based approach to predict the thermal performance of phase change material integrated building envelope. Building and Environment, 199, (2021) 107927. https://doi.org/10.1016/j.buildenv.2021.107927

[14] A. Basem, H.K. Abdulaali, A. Alizadeh, P.K. Singh, K. Parashar, A.E. Anqi, H. Rajab, P. Cajla, H. Maleki, Integrating artificial Intelligence-Based metaheuristic optimization with Machine learning to enhance Nanomaterial-Containing latent heat thermal energy storage systems. Energy Conversion and Management X, 25, (2025) 100835. https://doi.org/10.1016/j.ecmx.2024.100835

[15] R. Jia, K. Sun, R. Li, Y. Zhang, W. Wang, H. Yin, D. Fang, Q. Shi, Z. Tan, Heat capacities of some sugar alcohols as phase change materials for thermal energy storage applications. The Journal of Chemical Thermodynamics, 115, (2017) 233–248. https://doi.org/10.1016/j.jct.2017.08.004

[16] T. Wu, N. Xie, J. Niu, J. Luo, X. Gao, Y. Fang, Z. Zhang, Preparation of a low-temperature nanofluid phase change material: MgCl2–H2O eutectic salt solution system with multi-walled carbon nanotubes (MWCNTs). International Journal of Refrigeration, 113, (2020) 136–144. https://doi.org/10.1016/j.ijrefrig.2020.02.008

[17] R.P. Singh, S. Kaushik, D. Rakshit, Melting phenomenon in a finned thermal storage system with graphene nano-plates for medium temperature applications. Energy Conversion and Management, 163, (2018) 86–99. https://doi.org/10.1016/j.enconman.2018.02.053

[18] B. Dong, C. Cao, S.E. Lee, Applying support vector machines to predict building energy consumption in tropical region. Energy and Buildings, 37(5), (2004) 545–553. https://doi.org/10.1016/j.enbuild.2004.09.009

[19] L. Wei, W. Tian, E.A. Silva, R. Choudhary, Q. Meng, S. Yang, Comparative Study on Machine Learning for Urban Building Energy Analysis. Procedia Engineering, 121, (2015) 285–292. https://doi.org/10.1016/j.proeng.2015.08.1070

[20] H. Bagheri-Esfeh, H. Safikhani, S. Motahar, Multi-objective optimization of cooling and heating loads in residential buildings integrated with phase change materials using the artificial neural network and genetic algorithm. Journal of Energy Storage, 32, (2020) 101772. https://doi.org/10.1016/j.est.2020.101772

[21] Y. Lin, W. Yang, Application of Multi-Objective Genetic Algorithm Based Simulation for Cost-Effective Building Energy Efficiency Design and Thermal Comfort Improvement. Frontiers in Energy Research, 6, (2018) 25. https://doi.org/10.3389/fenrg.2018.00025

[22] X. Xiao, Q. Hu, H. Jiao, Y. Wang, A. Badiei, Simulation and machine learning investigation on thermoregulation performance of phase change walls. Sustainability, 15(14), (2023) 11365. https://doi.org/10.3390/su151411365

[23] L.G. Socaciu, P.V. Unguresan, Using the Analytic Hierarchy Process to Prioritize and Select Phase Change Materials for Comfort Application in Buildings. Scientific Journal. Series Mathematical Modelling in Civil Engineering, 10(1), (2014) 21–28. https://doi.org/10.2478/mmce-2014-0003

[24] P. Erdinç, Z. Buduneli, Ç. Gerşil, C. Erton, M. Paldrak, E. Staiou, (2024). Analytic Hierarchy Process (AHP) and Goal Programming Approach for a Real-Life Supplier Selection Problem. In Lecture notes in mechanical engineering, Springer. https://doi.org/10.1007/978-3-031-53991-6_53

[25] F. Nurprihatin, R. Antonius, G.D. Rembulan, R. Djajasoepena, E. Sulistyo, Analytical Hierarchy Process And Topsis Approach To Perform Supplier Selection In Construction Industry. Jiems (Journal of Industrial Engineering and Management Systems), 15(2), (2023). https://doi.org/10.30813/jiems.v15i2.4124

[26] F.M. Monticeli, R.M. Neves, H.L.O. Júnior, Using an artificial neural network (ANN) for prediction of thermal degradation from kinetics parameters of vegetable fibers. Cellulose, 28(4), (2021) 1961–1971. https://doi.org/10.1007/s10570-021-03684-2

[27] J.P. Martin, B.J. Rasor, J. DeBonis, A.S. Karim, M.C. Jewett, K.E. Tyo, L.J. Broadbelt, A dynamic kinetic model captures cell-free metabolism for improved butanol production. Metabolic Engineering, 76, (2023) 133–145. https://doi.org/10.1016/j.ymben.2023.01.009

[28] N.A. Van Riel, Dynamic modelling and analysis of biochemical networks: mechanism-based models and model-based experiments. Briefings in Bioinformatics, 7(4), (2006) 364–374. https://doi.org/10.1093/bib/bbl040

[29] K. Patidar, A. Singathia, M. Vashishtha, V. Kumar Sangal, S. Upadhyaya, Investigation of kinetic and thermodynamic parameters approaches to non-isothermal pyrolysis of mustard stalk using model-free and master plots methods. Materials Science for Energy Technologies, 5, (2022) 6-14. https://doi.org/10.1016/j.mset.2021.11.001

[30] E. Tarani, K. Chrissafis, Isoconversional methods: A powerful tool for kinetic analysis and the identification of experimental data quality. Thermochimica Acta, 733, (2024) 179690. https://doi.org/10.1016/j.tca.2024.179690

[31] L. Feng, J. Zheng, H. Yang, Y. Guo, W. Li, X. Li, Preparation and characterization of polyethylene glycol/active carbon composites as shape-stabilized phase change materials. Solar Energy Materials and Solar Cells, 95(2), (2011) 644-650. https://doi.org/10.1016/j.solmat.2010.09.033

[32] I.A. Laghari, M. Samykano, A. Pandey, Z. Said, K. Kadirgma, V. Tyagi, (2022). Thermal conductivity and Thermal properties enhancement of Paraffin/ Titanium Oxide based Nano enhanced Phase change materials for Energy storage. 2022 Advances in Science and Engineering Technology International Conferences (ASET), IEEE, Dubai, United Arab Emirates. https://doi.org/10.1109/aset53988.2022.9735037

[33] B.S. Jinshah, R.K. Kottala, K.R. Balasubramanian, A. Francis, Experimental analysis of phase change material integrated single phase natural circulation loop. Materials Today: Proceedings, 46, (2021) 10000-10005. https://doi.org/10.1016/j.matpr.2021.04.251

Authors Contribution Statement

K. Pavan Kumar: Conceptualization; Methodology; Investigation; Experimental work; Software and coding; Data curation; Formal analysis; Visualization; Original draft preparation. T.V.K. Bhanu Prakash: Conceptualization; Supervision; Project administration; Methodological guidance; Validation; Critical review and Writing, Review and Editing. Aditya Mukherjee: Supervision; Technical guidance; Writing, Review and Editing. All the authors read and approved the final version of the manuscript.

Funding

The authors declare that no funds, grants or any other support were received during the preparation of this manuscript.

Competing Interests

The authors declare that there are no conflicts of interest regarding the publication of this manuscript.

Data Availability

The experimental and model derived databases utilized in this work are available from the corresponding author upon request.

Has this article screened for similarity?

Yes